Article

A trade-off between plant and soil carbon storage under elevated CO_2

https://doi.org/10.1038/s41586-021-03306-8

Received: 16 July 2020

Accepted: 27 January 2021

Published online: 24 March 2021

Check for updates

C. Terrer[1,2]✉, R. P. Phillips[3], B. A. Hungate[4,5], J. Rosende[6], J. Pett-Ridge[1], M. E. Craig[3,7], K. J. van Groenigen[8], T. F. Keenan[9,10], B. N. Sulman[7], B. D. Stocker[11,12], P. B. Reich[13,14], A. F. A. Pellegrini[2,15], E. Pendall[14], H. Zhang[16], R. D. Evans[17], Y. Carrillo[14], J. B. Fisher[18,19], K. Van Sundert[20], Sara Vicca[20] & R. B. Jackson[2,21]

Terrestrial ecosystems remove about 30 per cent of the carbon dioxide (CO_2) emitted by human activities each year[1], yet the persistence of this carbon sink depends partly on how plant biomass and soil organic carbon (SOC) stocks respond to future increases in atmospheric CO_2 (refs. [2,3]). Although plant biomass often increases in elevated CO_2 (eCO_2) experiments[4–6], SOC has been observed to increase, remain unchanged or even decline[7]. The mechanisms that drive this variation across experiments remain poorly understood, creating uncertainty in climate projections[8,9]. Here we synthesized data from 108 eCO_2 experiments and found that the effect of eCO_2 on SOC stocks is best explained by a negative relationship with plant biomass: when plant biomass is strongly stimulated by eCO_2, SOC storage declines; conversely, when biomass is weakly stimulated, SOC storage increases. This trade-off appears to be related to plant nutrient acquisition, in which plants increase their biomass by mining the soil for nutrients, which decreases SOC storage. We found that, overall, SOC stocks increase with eCO_2 in grasslands (8 ± 2 per cent) but not in forests (0 ± 2 per cent), even though plant biomass in grasslands increase less (9 ± 3 per cent) than in forests (23 ± 2 per cent). Ecosystem models do not reproduce this trade-off, which implies that projections of SOC may need to be revised.

The future of the land sink, especially of SOC, is particularly uncertain[9]. Soils can become either sources or sinks of carbon with rising levels of atmospheric CO_2, depending on the prevalence of gains via photosynthesis or losses via respiration[9,10]. This uncertainty in terrestrial ecosystem model projections reflects uncertainty in both the mechanisms and the parameter values controlling SOC cycling under eCO_2[11].

Plant growth generally increases in response to eCO_2[4,12], with soil nutrients identified as the dominant factor explaining variability across experiments[12–15]. The effect of eCO_2 on SOC stocks (β_{soil}) is more equivocal. Although the expectation is that SOC will accrue as eCO_2 increases plant growth[16], a few experiments show increases in β_{soil}, many show no change, and some even show losses[7]. The observed variation in β_{soil} across experiments is puzzling, and there is wide disagreement regarding the dominant mechanisms explaining this variation[7,17,18].

A positive relationship between the effects of eCO_2 on plant biomass and SOC pools is expected if increased plant production under eCO_2 increases carbon inputs (litter) into the soil. Indeed, a positive relationship between inputs and SOC storage is formalized in first-order kinetics[16] and is applied in most terrestrial ecosystem models[19,20]. Because the effect of eCO_2 on plant aboveground biomass (β_{plant}) is strongly correlated with the effect of eCO_2 on litter production (Extended Data Fig. 1a, $r = 0.81$) and on root production[21], a positive relationship between β_{plant} and β_{soil} can thus be expected from first-order kinetics. This hypothesis, however, ignores SOC losses associated with accelerated soil organic matter decomposition sometimes observed under eCO_2[7,18]. Plants acquire limiting resources from soils through carbon investment belowground in root growth, exudates and symbiotic bacteria and fungi. Accelerated decomposition of soil organic matter fuelled by plant carbon inputs can enable plant nutrient uptake (the "priming effect"[22]). The return on this belowground carbon investment is an increase in aboveground biomass production[15]. However, the priming effect can decrease SOC[5]. A negative relationship between

[1]Physical and Life Sciences Directorate, Lawrence Livermore National Laboratory, Livermore, CA, USA. [2]Department of Earth System Science, Stanford University, Stanford, CA, USA. [3]Department of Biology, Indiana University, Bloomington, IN, USA. [4]Center for Ecosystem Science and Society, Northern Arizona University, Flagstaff, AZ, USA. [5]Department of Biological Sciences, Northern Arizona University, Flagstaff, AZ, USA. [6]Institut de Ciència i Tecnologia Ambientals, Universitat Autònoma de Barcelona, Barcelona, Spain. [7]Environmental Sciences Division and Climate Change Science Institute, Oak Ridge National Laboratory, Oak Ridge, TN, USA. [8]Department of Geography, College of Life and Environmental Sciences, University of Exeter, Exeter, UK. [9]Department of Environmental Science, Policy and Management, UC Berkeley, Berkeley, CA, USA. [10]Climate and Ecosystem Sciences Division, Lawrence Berkeley National Laboratory, Berkeley, CA, USA. [11]Department of Environmental Systems Science, ETH, Zürich, Switzerland. [12]Swiss Federal Institute for Forest, Snow and Landscape Research WSL, Birmensdorf, Switzerland. [13]Department of Forest Resources, University of Minnesota, St Paul, MN, USA. [14]Hawkesbury Institute for the Environment, Western Sydney University, Penrith, New South Wales, Australia. [15]Department of Plant Sciences, University of Cambridge, Cambridge, UK. [16]Environmental Change Institute, School of Geography and the Environment, University of Oxford, Oxford, UK. [17]School of Biological Sciences and the Stable Isotope Core Laboratory, Washington State University, Pullman, WA, USA. [18]Jet Propulsion Laboratory, California Institute of Technology, Pasadena, CA, USA. [19]Joint Institute for Regional Earth System Science and Engineering, University of California at Los Angeles, Los Angeles, CA, USA. [20]Plants and Ecosystems (PLECO), Biology Department, University of Antwerp, Wilrijk, Belgium. [21]Woods Institute for the Environment and Precourt Institute for Energy, Stanford University, Stanford, CA, USA. ✉e-mail: terrer@stanford.edu

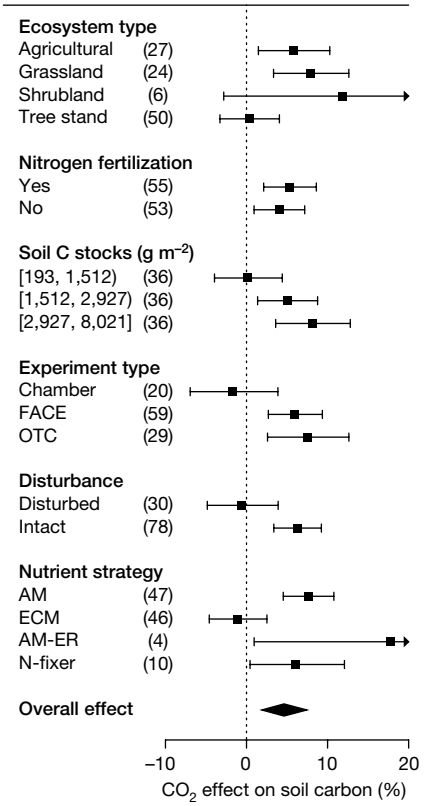

Fig. 1 | Meta-analysis of the effect of eCO_2 on percentage SOC across different factors. $n = 108$. Overall means and 95% confidence intervals are given; we interpret CO_2 effects when the zero line is not crossed by the confidence intervals. Arrows represent 95% confidence intervals that extend beyond the limits of the plot. Soil carbon stocks represent values in ambient CO_2 plots as a continuous variable, here expressed as intervals of equal sample size for illustration purposes. Values in parentheses are sample sizes. CO_2 effects represent, on average, an increase in CO_2 from 372 parts per million (ppm) to 616 ppm. FACE, Free Air CO_2 Enrichment; OTC, Open Top Chamber; AM-ER, mix of AM and ericoid mycorrhizal; N-fixer, fixation of atmospheric nitrogen.

β_{plant} and β_{soil} may thus emerge through the economics of plant resource acquisition.

Here, we evaluate the mechanisms of β_{soil}, including its relationship with β_{plant}, by synthesizing 268 observations of β_{soil} from 108 eCO_2 experiments spanning the globe with coupled β_{plant}–β_{soil} data (Supplementary Table 1) using meta-analysis techniques. We explore how well these mechanisms are represented in ecosystem models, and scale up the geographical distribution of β_{soil} derived from experiments to identify regions where models might be missing important processes.

Predictors of SOC accrual under eCO_2

Overall, eCO_2 increased SOC stocks by 4.6% across experiments (Fig. 1; 1.7% to 7.5%, 95% confidence interval, CI). Given the strong variation in β_{soil} across factors (Fig. 1), we used a random-forest approach in the context of meta-analysis (meta-forest) to quantify the importance of 19 potential predictors (Extended Data Table 1), including climate, soil, plant and ecosystem variables and their interactions, accounting for covariation across predictors and potential nonlinearities.

We found that β_{plant} is the most important predictor of β_{soil} (Extended Data Fig. 2a, b; $n = 108$), revealing a strong coupling between CO_2-driven changes in plant biomass and SOC. In addition, β_{soil} increased with background SOC stocks (Fig. 1), also identified as an important predictor.

Contrary to expectations from some first-order models[19,20], the relationship between β_{soil} and β_{plant} was negative. For the subset ($n = 73$) of field experiments with intact soils (non-potted plants and non-reconstructed soils), we found a significant interaction between β_{plant} and nitrogen (N) fertilization (Extended Data Fig. 2c; $P < 0.01$). In non-fertilized experiments, the slope between β_{soil} and β_{plant} was significantly negative (Fig. 2a; $P < 0.0001$, $R^2 = 0.67$, $n = 38$), whereas in fertilized experiments the slope was less pronounced and not significant ($P = 0.34$, $n = 35$) (Extended Data Fig. 3a). In non-fertilized experiments, increases in plant biomass were associated with decreasing SOC stocks (Fig. 2a), consistent with the priming effect. In N-fertilized experiments, eCO_2 generally increased both plant biomass and SOC (Extended Data Fig. 3b), in line with first-order kinetics.

We propose a framework to explain the negative relationship between β_{soil} and β_{plant}, based on plant nutrient acquisition strategies.

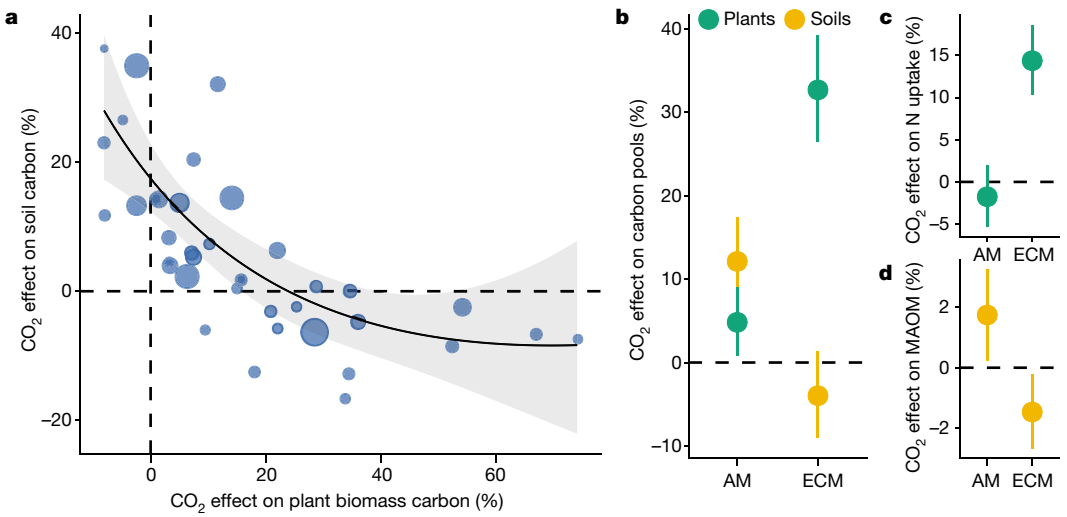

Fig. 2 | Elevated CO_2 experiments show an inverse relationship between the effects of eCO_2 on plant biomass and SOC stocks due to plant nutrient-acquisition. This inverse relationship (**a**) can be explained by the different efficiencies in plant nutrient uptake (**c**) between AM and ECM nutrient-acquisition strategies driving opposite effects on plant biomass and SOC pools (**b**), including MAOM stocks (**d**). The regression line in **a** is based on a quadratic mixed-effects meta-regression model and 95% confidence interval ($R^2 = 0.67$, $P < 0.0001$, $n = 38$). Dots in **a** represent the individual experiments in the meta-analysis, with dot sizes proportional to model weights. Dots in **b**–**d** represent overall effect sizes from a meta-analysis and 95% confidence intervals. Data shown here are for non-fertilized experiments (see Extended Data Fig. 3 for nutrient-fertilized experiments).

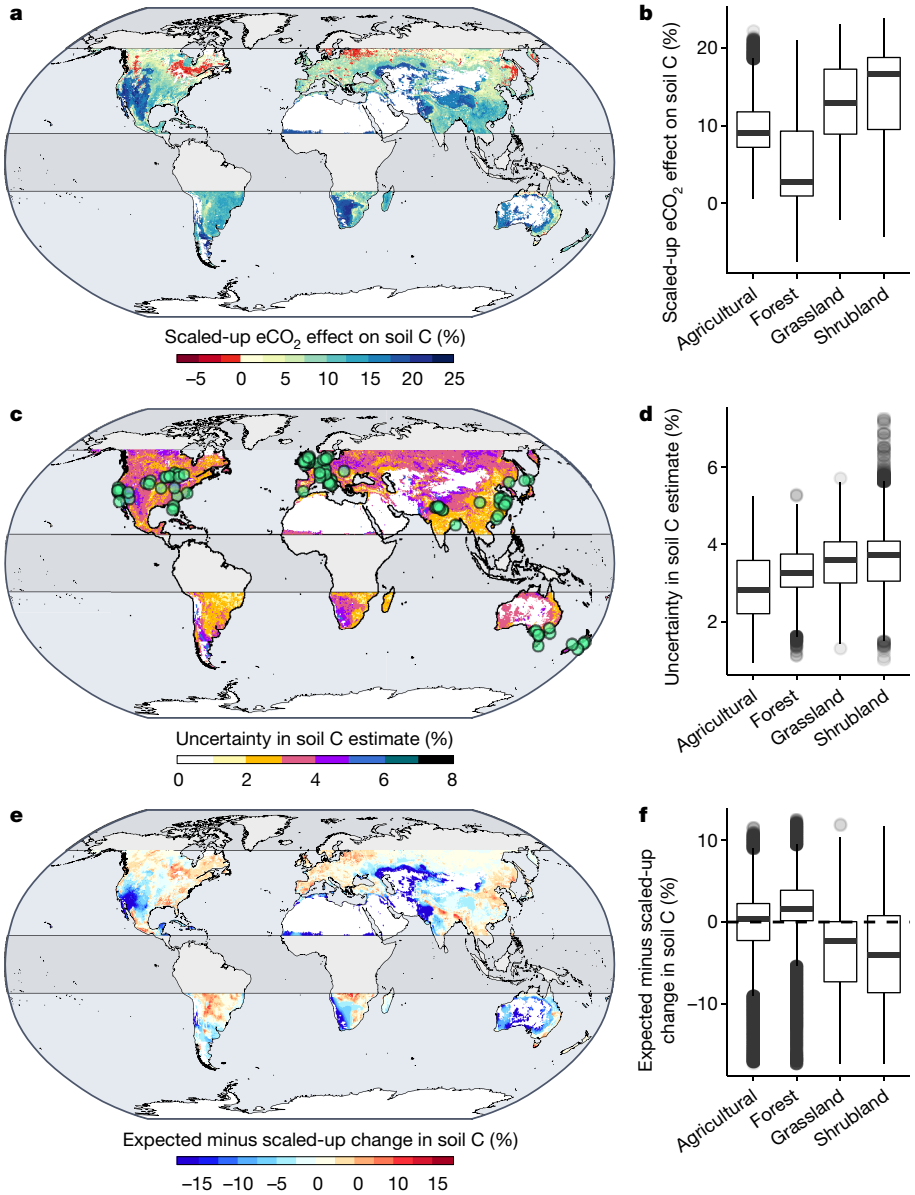

Fig. 3 | Effect of eCO_2 (about 240 ppm) on SOC stocks scaled up from 108 CO_2 experiments. **a**, **b**, Relative effect of elevated CO_2 on SOC scaled up on the basis of a meta-forest approach with data from CO_2 experiments, with the spatial distribution shown on a map (**a**) and aggregated by ecosystem type (**b**). **c** shows the standard error in **a**, and **d** shows the standard error in **b**. Green dots in **c** represent the location of the CO_2 experiments included in the analysis. **e**, **f**, Difference between expected CO_2 effects on SOC stocks based on CMIP5 models and scaled up on the basis of experiments (shown in **a**) with the spatial distribution shown on a map (**e**) and aggregated by ecosystem type (**f**). Expected values result from the relationship between β_{soil} and β_{plant} coded in models. Positive values (reddish colours) indicate an overestimation by models; negative values (bluish colours) indicate an underestimation by models. Shaded areas between −15 to 15 and from 60° to 90° in latitude represent ecosystems not well sampled by experiments that we excluded from the analysis. Boxplots show the median, the first to third quartile, the 1.5× interquartile ranges, and outliers. On average, the difference between elevated CO_2 and control plots in the experiments is 240 ppm.

Symbiotic associations between plants and fungi—arbuscular mycorrhizae (AM) and ectomycorrhizae (ECM)—mediate β_{plant} (Extended Data Fig. 2d), resulting in much higher β_{plant} in ECM-associated plants than in AM-associated plants when nutrient availability is low (Fig. 2b). ECM-associated plants efficiently increase N uptake under eCO_2 (Fig. 2c; $n = 12$), enhancing β_{plant}. However, acquiring N from soil organic matter via priming accelerates SOC losses[7], reducing β_{soil} in ECM (Fig. 2b). In contrast, eCO_2 did not significantly affect N uptake in AM systems (Fig. 2c; $n = 12$, $P = 0.3460$). This outcome limits β_{plant} in AM systems but stimulates β_{soil} (Fig. 2b), probably owing to increased carbon inputs through fine-root production and rhizodeposition[21,23,24] combined with decreased carbon losses[25]. The composition of the soil organic matter may mediate this effect as well: AM plants produce more easily decomposable litter[26], which enhances mineral-associated soil organic matter (MAOM) formation[27] and results in a greater fraction of SOC in MAOM under AM relative to ECM systems[28,29]. Indeed, eCO_2 increases MAOM more strongly in AM systems than in ECM systems (Fig. 2d; $n = 19$). Because MAOM is less accessible to microbial decomposers[30], greater MAOM in AM systems could limit priming-induced losses and promote long-term SOC storage.

We considered three alternative mechanisms that could potentially explain this trade-off. First, grasses allocate more carbon to roots than trees, which is associated with greater SOC stocks[31,32]. Because grassland species associate with AM fungi and the majority of tree species in the dataset associate with ECM, the observed increase in β_{soil} in AM systems could be driven by ecosystem type rather than mycorrhizal type. However, we found that eCO_2 effects on root biomass and fine-root production were generally lower in grasses than trees, and were also lower in AM-associated than in ECM-associated trees (Extended Data Fig. 4). Second, in non-fertilized experiments with available data ($n = 16$), eCO_2 increased litter C:N by 8%, which could reduce the decomposability of litter and the stabilization of carbon in the soil[27]. If litter quality is reduced more in ECM systems than in AM systems, this could help explain why eCO_2 increased SOC in AM systems, but not in ECM systems. However, the effect of eCO_2 on litter quality was similar between mycorrhizal types (Extended Data Fig. 4). Finally, contrasting β_{soil} in AM systems versus ECM systems could be driven by larger background SOC in grasslands than in forests, given that higher SOC is associated with higher β_{soil} (Fig. 1). We found, however, that background SOC was similar between mycorrhizal types and ecosystem types (Extended Data Fig. 4). Thus, differences in root allocation, litter quality and background SOC in grasses versus trees cannot explain the trade-off between β_{soil} and β_{plant}. Instead, losses in SOC associated with plant

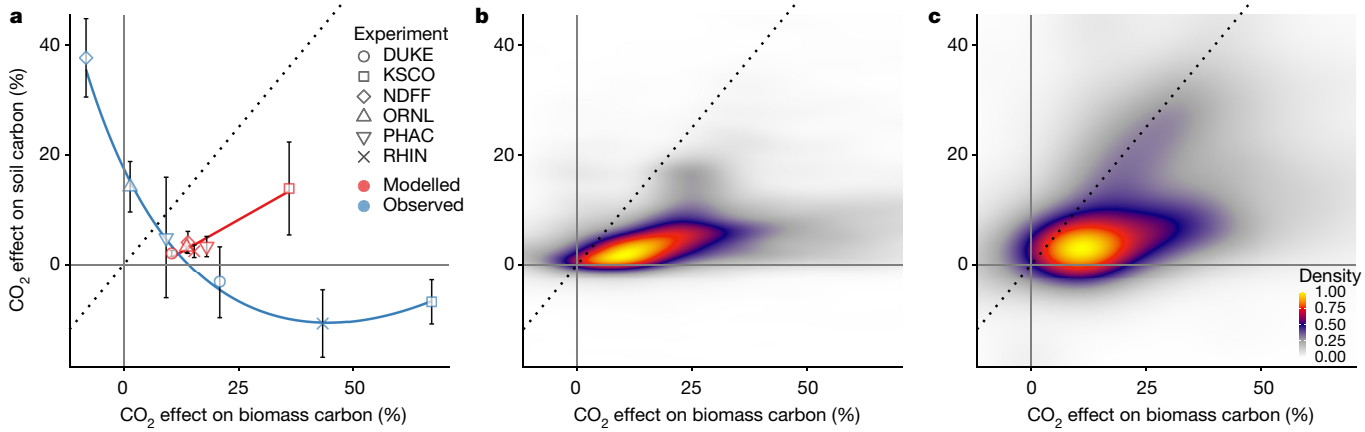

Fig. 4 | Comparison of modelled and measured relationships between aboveground biomass and SOC responses to CO_2. a, Relationship observed (blue) and modelled (red) across six eCO_2 experiments. Model results are based on 12 models applied to the same six experiments with a common forcing and initialization protocol. The experiments included are: Duke FACE (DUKE), Kennedy Space Center (KSCO), Nevada Desert FACE (NDFF), Oak Ridge FACE (ORNL), Prairie PHACE (PHAC), and Rhinelander (RHIN). The regression line across observations in **a** is based on a quadratic meta-regression model. Modelled simulations averaged in **a** for each experiment are from the FACE-MDS project phase 2 (ref. [34]). **b**, **c**, Global-scale relationship simulated by ecosystem models from the TRENDY ensemble for the historical increase in CO_2 since the year 1700 (**b**) and from the CMIP5 ensemble for an increase in CO_2 from 372 ppm to 616 ppm as in eCO_2 experiments (**c**). Dotted lines are the 1:1 line.

nutrient uptake (priming effect) in ECM systems, and gains associated with rhizodeposition in AM systems, are probably essential. Experiments including both AM-associated and ECM-associated tree species should be targeted to better understand the impacts of nutrient-acquisition strategies under eCO_2.

Scaling up

To explore the potential geographical distribution of β_{soil}, we simulated a global free-air CO_2 enrichment (FACE) experiment (Fig. 3a)[12]. Unlike Fig. 1, in which predictors are analysed individually, our meta-forest model can scale up β_{soil} from experiments while accounting for all important predictors simultaneously on a grid (Extended Data Figs. 5, 6; tenfold cross-validated $R^2 = 0.51$). Grasslands, croplands and shrublands showed a stronger potential to accumulate SOC in response to experimental eCO_2 than did forests (Fig. 3a, b). Soils in semi-arid herbaceous ecosystems were particularly responsive to eCO_2, consistent with the results from the Mojave desert FACE experiment that showed eCO_2-driven increases in SOC, but not biomass[33]. We identified large areas not currently sampled with eCO_2 experiments, particularly in the tropics and high latitudes (Fig. 3c, d, Extended Data Fig. 6), where new experiments would help to reduce uncertainties.

Data–model comparison

In addition to the negative relationship between β_{soil} and β_{plant}, we also found a significantly negative relationship between β_{soil} and the effect of eCO_2 on aboveground biomass production (Extended Data Fig. 1b; $R^2 = 0.55$, $P < 0.001$), which is strongly correlated with litter production (Extended Data Fig. 1a; $R^2 = 0.63$, $r = 0.81$, $P < 0.01$). This result questions the positive relationship between litter inputs and SOC stocks encoded in most ecosystem models. Thus, we investigated the relationship between β_{soil} and β_{plant} in models from three different model ensembles (description in Extended Data Table 2). First, models from the FACE-MDS project[34] mimic the experimental treatment in six eCO_2 experiments and allow for a direct comparison with respective observations. Although observations from the six experiments included in FACE-MDS showed a negative relationship between β_{soil} and β_{plant} (blue line in Fig. 4a; $R^2 = 0.99$, $P < 0.001$), the twelve models simulated a positive relationship when pooled by experiment (red line in Fig. 4a; $R^2 = 0.91$, $P < 0.01$). The relationship across all models individually was positive as well (dashed line in Extended Data Fig. 7a; $R^2 = 0.37$, $P < 0.0001$), and none of the individual models was able to reproduce the observations. Second, to investigate whether the same relationships emerge across the globe and in simulations where CO_2 increases gradually, we evaluated global century-scale relationships between β_{soil} and β_{plant} from the TRENDY and CMIP5 model ensembles (Fig. 4b, c). Overall, TRENDY and CMIP5 models did not simulate a negative relationship either (Fig. 4b, c). Instead, most models simulated a positive relationship and the vast majority of model simulations fell into the upper-right quadrant of CO_2 effect on SOC storage plotted against CO_2 effect on biomass carbon (Extended Data Fig. 7b, c), reflecting that inputs drive SOC accumulation in the first-order soil decomposition structure common to the models.

In TRENDY and CMIP5 model simulations, β_{soil} was estimated over a much longer time period than in experiments (Extended Data Table 2). Given the relatively slow turnover times of SOC pools, and the slow pace of changes in species composition and evolutionary pressures on both plants and soil microbes, long-term effects are likely to differ from those found in experiments. However, first-order models simulate a positive relationship β_{plant}:β_{soil} when they are forced to simulate the temporal scale of experiments (Fig. 4a), suggesting that important processes are missing in models. By including explicit links between plant growth, belowground carbon allocation and SOC decomposition rates, models may more effectively reproduce the observed negative relationship between β_{soil} and β_{plant} and improve long-term projections.

To estimate the error in terrestrial ecosystem model projections of β_{soil} caused by ignoring the trade-off between β_{soil} and β_{plant}, we calculated the 'expected' β_{soil} as a function of our scaled-up β_{plant} and the ratio $\beta_{soil}/\beta_{plant}$ simulated by CMIP5 models. CMIP5 models overestimated β_{soil} for forests (reddish shades in Fig. 3e, f). In contrast, CMIP5 models underestimated β_{soil} in large areas dominated by grasses (bluish shades in Fig. 3e, f), probably because they do not account for the effects of rhizodeposition on β_{soil} (ref. [21]). Results with TRENDY models were similar (Extended Data Fig. 8).

Discussion

In summary, our synthesis of experiments shows that SOC stocks can increase by approximately 5% in response to a 65% step increase in CO_2

concentrations, with a strong coupling between CO_2-driven changes in plant aboveground biomass and SOC. However, the coupling between plant biomass and soils is an inverse relationship (Fig. 2a, Extended Data Fig. 1b), opposite to that simulated by many ecosystem models (Fig. 4). The effect of eCO_2 on SOC storage is dependent on a fine balance between changes in inputs and changes in turnover[18], where the latter is dependent on root–microbe–mineral interactions in the rhizosphere. Our results suggest that rhizosphere responses, and especially priming, explain much of the variation in β_{soil} across experiments (Fig. 2). Most models focus on carbon inputs and underestimate rhizosphere effects[11,20,35], probably explaining the disagreement in β_{soil} between observations and models (Figs. 3, 4). We propose a framework to explain β_{soil} based on nutrient acquisition strategies[15,36,37]. On one end of the spectrum, substantial acquisition of soil N is possible via priming[5] in ECM-associated plants, causing a stronger plant biomass sink at the expense of SOC accrual. On the other end, low nutrient availability strongly constrains the plant biomass sink[38] in AM-associated plants. However, the ecosystem-level sink is not necessarily eliminated; instead, eCO_2 can trigger SOC accrual through plant carbon allocation belowground[21,23,24]. When plant growth is severely limited by N or other nutrients, eCO_2 may cause only a transient priming effect in ECM systems with high soil decomposition and insufficient plant nutrient uptake producing no ecosystem-level sink[39].

Our results emphasize the potential of grassland soils to store carbon as atmospheric CO_2 levels continue to rise. The results also suggest that state-of-the-art models may overestimate the SOC sequestration potential of forests in large parts of the world. Previous studies suggest that the potential of vegetation to take up CO_2 will slow later this century owing to nutrient constraints[12–14,38,39]. Our synthesis indicates that these nutrient constraints extend to carbon storage in ecosystems as a whole—through a partial tradeoff between increased plant growth and SOC storage, whereby ecosystems where plant growth is more nutrient-limited accumulate more carbon belowground. The apparent mismatch between observations and how most models represent the biomass-to-soil link suggests that many terrestrial ecosystem models do not adequately represent the critical processes driving SOC accumulation. Models are evolving to include more sophisticated representations of soil nutrient cycling, and some now include microbial activity explicitly[36,40]. This change towards coupled carbon-nutrient cycling mediated by plant–soil interactions is important for more realistic and accurate modelling of the carbon cycle today and for projecting the land sink in the future.

Online content

Any methods, additional references, Nature Research reporting summaries, source data, extended data, supplementary information, acknowledgements, peer review information; details of author contributions and competing interests; and statements of data and code availability are available at https://doi.org/10.1038/s41586-021-03306-8.

1. Friedlingstein, P. et al. Global carbon budget 2020. *Earth Syst. Sci. Data* **12**, 3269–3340 (2020).
2. Schimel, D., Stephens, B. B. & Fisher, J. B. Effect of increasing CO_2 on the terrestrial carbon cycle. *Proc. Natl Acad. Sci. USA* **112**, 436–441 (2015).
3. Keenan, T. et al. Recent pause in the growth rate of atmospheric CO_2 due to enhanced terrestrial carbon uptake. *Nat. Commun.* **7**, 13428 (2016).
4. Baig, S., Medlyn, B. E., Mercado, L. M. & Zaehle, S. Does the growth response of woody plants to elevated CO_2 increase with temperature? A model-oriented meta-analysis. *Glob. Change Biol.* **21**, 4303–4319 (2015).
5. Drake, J. E. et al. Increases in the flux of carbon belowground stimulate nitrogen uptake and sustain the long-term enhancement of forest productivity under elevated CO_2. *Ecol. Lett.* **14**, 349–357 (2011).
6. Norby, R. J. et al. Forest response to elevated CO_2 is conserved across a broad range of productivity. *Proc. Natl Acad. Sci. USA* **102**, 18052–18056 (2005).
7. van Groenigen, K. J., Qi, X., Osenberg, C. W., Luo, Y. & Hungate, B. A. Faster decomposition under increased atmospheric CO_2 limits soil carbon storage. *Science* **344**, 508 (2014).
8. Friedlingstein, P. et al. Uncertainties in CMIP5 climate projections due to carbon cycle feedbacks. *J. Clim.* **27**, 511–526 (2014).
9. Todd-Brown, K. E. O. et al. Changes in soil organic carbon storage predicted by Earth system models during the 21st century. *Biogeosciences* **11**, 2341–2356 (2014).
10. Heimann, M. & Reichstein, M. Terrestrial ecosystem carbon dynamics and climate feedbacks. *Nature* **451**, 289–292 (2008).
11. Bradford, M. A. et al. Managing uncertainty in soil carbon feedbacks to climate change. *Nat. Clim. Chang.* **6**, 751–758 (2016).
12. Terrer, C. et al. Nitrogen and phosphorus constrain the CO_2 fertilization of global plant biomass. *Nat. Clim. Chang.* **9**, 684–689 (2019).
13. Reich, P. B., Hungate, B. A. & Luo, Y. Carbon-nitrogen interactions in terrestrial ecosystems in response to rising atmospheric carbon dioxide. *Annu. Rev. Ecol. Evol. Syst.* **37**, 611–636 (2006).
14. Norby, R. J. & Zak, D. R. Ecological lessons from free-air CO_2 enrichment (FACE) experiments. *Annu. Rev. Ecol.* **42**, 181–203 (2011).
15. Terrer, C. et al. Ecosystem responses to elevated CO_2 governed by plant–soil interactions and the cost of nitrogen acquisition. *New Phytol.* **217**, 507–522 (2018).
16. Olson, J. S. Energy storage and the balance of producers and decomposers in ecological systems. *Ecology* **44**, 322–331 (1963).
17. Hungate, B. A. et al. Assessing the effect of elevated carbon dioxide on soil carbon: a comparison of four meta-analyses. *Glob. Change Biol.* **15**, 2020–2034 (2009).
18. Kuzyakov, Y., Horwath, W. R., Dorodnikov, M. & Blagodatskaya, E. Review and synthesis of the effects of elevated atmospheric CO_2 on soil processes: no changes in pools, but increased fluxes and accelerated cycles. *Soil Biol. Biochem.* **128**, 66–78 (2019).
19. Tian, H. et al. Global patterns and controls of soil organic carbon dynamics as simulated by multiple terrestrial biosphere models: current status and future directions. *Glob. Biogeochem. Cycles* **29**, 775–792 (2015).
20. Todd-Brown, K. E. O. et al. Causes of variation in soil carbon simulations from CMIP5 Earth system models and comparison with observations. *Biogeosciences* **10**, 1717–1736 (2013).
21. Nie, M., Lu, M., Bell, J., Raut, S. & Pendall, E. Altered root traits due to elevated CO_2: a meta-analysis. *Glob. Ecol. Biogeogr.* **22**, 1095–1105 (2013).
22. Kuzyakov, Y. Priming effects: interactions between living and dead organic matter. *Soil Biol. Biochem.* **42**, 1363–1371 (2010).
23. Treseder, K. K. A meta-analysis of mycorrhizal responses to nitrogen, phosphorus, and atmospheric CO_2 in field studies. *New Phytol.* **164**, 347–355 (2004).
24. Jastrow, J. D. et al. Elevated atmospheric carbon dioxide increases soil carbon. *Glob. Change Biol.* **11**, 2057–2064 (2005).
25. Carrillo, Y., Dijkstra, F. A., LeCain, D. & Pendall, E. Mediation of soil C decomposition by arbuscular mycorrizhal fungi in grass rhizospheres under elevated CO_2. *Biogeochemistry* **127**, 45–55 (2016).
26. Averill, C., Bhatnagar, J. M., Dietze, M. C., Pearse, W. D. & Kivlin, S. N. Global imprint of mycorrhizal fungi on whole-plant nutrient economics. *Proc. Natl Acad. Sci. USA* **116**, 23163–23168 (2019).
27. Cotrufo, M. F., Wallenstein, M. D., Boot, C. M., Denef, K. & Paul, E. The Microbial Efficiency-Matrix Stabilization (MEMS) framework integrates plant litter decomposition with soil organic matter stabilization: do labile plant inputs form stable soil organic matter? *Glob. Change Biol.* **19**, 988–995 (2013).
28. Cotrufo, M. F., Ranalli, M. G., Haddix, M. L., Six, J. & Lugato, E. Soil carbon storage informed by particulate and mineral-associated organic matter. *Nat. Geosci.* **12**, 989–994 (2019).
29. Craig, M. E. et al. Tree mycorrhizal type predicts within-site variability in the storage and distribution of soil organic matter. *Glob. Change Biol.* **24**, 3317–3330 (2018).
30. Schmidt, M. W. I. et al. Persistence of soil organic matter as an ecosystem property. *Nature* **478**, 49–56 (2011).
31. Jobbágy, E. G. & Jackson, R. B. The vertical distribution of soil organic carbon and its relation to climate and vegetation. *Ecol. Appl.* **10**, 423–436 (2000).
32. Sokol, N. W., Kuebbing, S. E., Karlsen-Ayala, E. & Bradford, M. A. Evidence for the primacy of living root inputs, not root or shoot litter, in forming soil organic carbon. *New Phytol.* **221**, 233–246 (2019).
33. Evans, R. D. et al. Greater ecosystem carbon in the Mojave Desert after ten years exposure to elevated CO_2. *Nat. Clim. Chang.* **4**, 394–397 (2014).
34. Walker, A. P. et al. *FACE-MDS Phase 2: Model Output* https://www.osti.gov/dataexplorer/biblio/dataset/1480327 (2018).
35. Wieder, W. R. et al. Carbon cycle confidence and uncertainty: exploring variation among soil biogeochemical models. *Glob. Change Biol.* **24**, 1563–1579 (2018).
36. Sulman, B. N. et al. Diverse mycorrhizal associations enhance terrestrial C storage in a global model. *Glob. Biogeochem. Cycles* **33**, 501–523 (2019).
37. Shi, M., Fisher, J. B., Brzostek, E. R. & Phillips, R. P. Carbon cost of plant nitrogen acquisition: global carbon cycle impact from an improved plant nitrogen cycle in the Community Land Model. *Glob. Change Biol.* **22**, 1299–1314 (2016).
38. Norby, R. J., Warren, J. M., Iversen, C. M., Medlyn, B. E. & McMurtrie, R. E. CO_2 enhancement of forest productivity constrained by limited nitrogen availability. *Proc. Natl Acad. Sci. USA* **107**, 19368–19373 (2010).
39. Jiang, M. et al. The fate of carbon in a mature forest under carbon dioxide enrichment. *Nature* **580**, 227–231 (2020).
40. Wieder, W. R., Bonan, G. B. & Allison, S. D. Global soil carbon projections are improved by modelling microbial processes. *Nat. Clim. Chang.* **3**, 909–912 (2013).

Publisher's note Springer Nature remains neutral with regard to jurisdictional claims in published maps and institutional affiliations.

© This is a U.S. government work and not under copyright protection in the U.S.; foreign copyright protection may apply 2021

Methods

Overview

Here, we collect data on the effects of eCO_2 on SOC stocks (β_{soil}) in both relative and absolute terms and synthesize them through meta-analysis. We also collect data on climatic, experimental and vegetation characteristics that could potentially explain variability in β_{soil} ('predictors'). In Fig. 1, we show a descriptive meta-analysis of overall β_{soil} across different predictor factors. We next combine the strengths of meta-analysis (for example, accounting for within-study variability, weights) with random-forest (for example, computational efficiency, nonlinearities, interactions)—that is, meta-forest—to quantify the relative importance of 19 predictors in explaining variation in β_{soil} in the dataset. In Fig. 2, we describe the regression between β_{soil} and its most important predictor (β_{plant}), and explore the possible mechanisms underlying this relationship. In Fig. 3, we apply the data-trained meta-forest model to scale up β_{soil}. Finally, we investigate whether the emerging relationship between β_{soil} and β_{plant} found in experiments is represented in models (Fig. 4).

Data collection

We compiled the publicly available Report of Mutualistic Associations, Nutrients, and Carbon under eCO_2 (ROMANCE) version 1.0 dataset[41] with data on SOC and plant biomass from eCO_2 experiments. Expanding van Groenigen et al.'s 2014 meta-analysis[7] of 53 experiments reporting SOC data, we used Google Scholar to gather a total of 166 studies related to eCO_2 experiments, published from 1 January 2013 to 1 May 2019. Search terms were either "elevated CO_2", "increased CO_2" or "CO_2 enrichment" and either "soil carbon" or "plant biomass". To account for experiments that could have been omitted by van Groenigen et al. before 2013, we consulted the Global List of FACE Experiments from the Oak Ridge National Laboratory (http://facedata.ornl.gov/global_face.html) and the database described by Dieleman et al.[42]. We recorded the structure of each eCO_2 experiment from the papers, taking into consideration the start date and total duration of the experiment (years), and the location of the experiment (coordinates). When the data were presented in figures, mean values and standard error were extracted using WebPlotDigitizer (https://automeris.io/WebPlotDigitizer/).

For this meta-analysis, only one datum per experiment was considered to avoid pseudoreplication. The effects of eCO_2 on soil C pools are modulated by increases in soil C inputs from plant litter as well as feedbacks between plants and soils altering soil biogeochemical cycles that can take several years to occur. Thus, we used the most recent measurements in each experiment as the most representative data of the effect of eCO_2 on SOC.

For plant biomass, measurements across different time points were combined so that only one effect size was analysed per study. The combined effect size and variance that account for the correlation among the different time-point measurements was calculated following the method described in Borenstein et al.[43], using a conservative approach by assuming non-independency of multiple outcomes ($r = 1$) and performed using the MAd package in R[44]. We collected data on both aboveground biomass stocks and production. When aboveground biomass production data were unavailable, we collected plant data in the following order of preference: net primary productivity, aboveground biomass increment, foliage production and yield. When biomass or soil data were not reported, studies were excluded. We also included the data on litter production reported by Song and Wan[45] to study the interactions with aboveground biomass and production data.

Soil carbon measurements in the dataset were reported at different depths, varying from 5 cm to 30 cm maximum depth, with an average depth of about 20 cm. When scaling up eCO_2 effects on SOC through meta-forest, we included a fixed value of 0–30 cm in depth as a covariate to control for the influence of soil depth, interpolating predictions for the same soil depth of models. SOC data reported in concentration were transformed to stocks (in grams per square metre) using soil bulk density. When bulk density was not reported, we used data reported for similar experiments within the same site or assumed a bulk density of 1 g cm^{-3}. Assumptions are indicated in the dataset.

Studies from ROMANCE version 1.0 were not included in the meta-analysis if they met any of the following exclusion criteria: (1) studies with no SOC data; (2) papers with no plant biomass data; (3) studies where the duration of the eCO_2 experiment lasted less than 0.5 yr. A total of 138 independent experiments were collected, of which 108 were included in the final analysis based on these exclusion criteria.

Meta-analysis

Two types of effect size were calculated: (1) the log response ratio (mean response in elevated-to-ambient CO_2 plots), to measure effect sizes in relative terms (in percentage) for each experiment; and (2) the raw mean difference, to compute effect sizes in absolute terms (in units of grams per square metre). For each experiment, we collected data on SOC stocks, standard deviation and sample size under elevated and ambient (control) CO_2 plots. Effect sizes were calculated using the *escalc* function from the R package *metafor*[46]. We calculated overall effects in a weighted, mixed-effects model using the *rma.mv* function in *metafor*. The potential non-independency of studies within the same site (for example, different species, different treatments) was accounted for by including 'site' as a random effect. Effect size measurements from individual studies in the meta-analysis were weighted by the inverse of the variance[47]. Standard deviations were not reported in 13% of the studies, and were thus imputed using Rubin and Schenker's[48] resampling approach from studies with similar means. These calculations were performed using the R package *metagear*[49].

Varying importance and scaling-up approach

We coded 19 potential moderators (Extended Data Table 1). Including all 19 moderators in a meta-regression risks overfitting the model, so we applied the R package *metaforest*[50] to identify potentially relevant moderators in predicting β_{soil} across the complete dataset of 108 studies. The approach is based on the machine-learning 'random forest' algorithm, which is robust to overfitting, and is integrated in a meta-analytic context by incorporating the variance and weight of each experiment as in classic meta-analysis (see above).

As an initial step, we conducted variable pre-selection by including the 19 predictors in *metaforest* with 10,000 iterations and replicated 100 times with a recursive algorithm in the *preselect* function from *metafor*[46]. Moderators that consistently displayed negative variable importance (that is, that showed a reduction in predictive performance) were dropped using the *preselect_vars* function. Moderators that improved predictive performance were then carried forward to optimize the model. Parameters of the meta-forest model were optimized using the *train* function from the *caret* package[51], and we calculated tenfold cross-validated R^2 with 75% of the data used as training data and 25% for validation. Unlike maximum likelihood model-selection approaches, this method can handle many potential predictors and their interactions and considers nonlinear relationships. Partial dependence plots were produced that visualize the association of each moderator with the effect size, while accounting for the average effect of all other moderators.

As a sensitivity test, and to identify important interactions between predictors, we ran an alternative model-selection procedure using maximum likelihood estimation. For this purpose, we used the *rma.mv()* function from the *metafor* R package[46] and the *glmulti()* function from the *glmulti* R package[52] to automate fitting of all possible models containing the five most important predictors and their interactions (at level 2). Model selection was based on Akaike Information Criterion corrected for small samples (AICc), with the relative importance value for a particular predictor equal to the sum of the Akaike weights (the probability that a model is the most plausible model) for the models in which the predictor appears.

Finally, the data-trained meta-forest model was applied to global gridded data of pre-selected predictors (see Extended Data Table 1 for

gridded data sources) to estimate the effect of elevated CO_2 on SOC. The resulting global maps are geographically constrained to ecosystems best represented by experiments. We remove the estimates for latitudes comprised between −15° and 15°, corresponding to tropical ecosystems not sampled by experiments (green dots in Fig. 3c), and from 60° to 90°.

Nitrogen fertilization and soil disturbance

We used the information reported in the papers to assess whether the soils were exposed to external inputs of N fertilization (yes) or not (no). Experiments were also classified as either having 'disturbed' or 'intact' soils as noted in the papers. If not, experiments that used pots or reconstructed soils were categorized as 'disturbed'. We used the same approach and classification as in ref. [53].

To scale up the effect of nitrogen fertilization and disturbance on β_{soil}, we reclassified the ESA CCI land cover map: http://www.esa-landcover-cci.org/. Reclassification files are available from: https://figshare.com/articles/dataset/Reclassification_of_ESA_land_cover/11710155. For example, we classify 'Cropland, rainfed' to 'Herbaceous cover' (class 11) and 'Cropland, irrigated or post-flooding' (class 20) as 'fertilized'.

Nutrient-acquisition strategy classification

We considered the importance of the type of symbiotic association as a driver of eCO_2 effects on soil C. Mycorrhizal status includes AM, ECM and a mix of AM and ER mycorrhizal plant–fungal associations. Here we also considered some plant species known to associate with N-fixing microorganisms. We refer to this classification as 'symbiotic', because it includes both mycorrhizal status and N-fixation. Together, these four symbiosis types represent different mechanisms plants use to acquire nutrients[15].

We assessed the impact of the dominant symbiotic association type by classifying all studies as ECM, AM, AM-ER and N-fixers, using the checklists by Wang et al.[54] and Maherali et al.[55], with additional classifications derived from the literature. Species that associate with both ECM and AM (for example, *Populus* spp.) were classified as ECM because these species can potentially benefit from increased N-availability owing to the presence of ECM fungi[56]. Most of the N-fixers in the dataset were associated with both N-fixing symbionts as well as AM fungi, but we classified them as N-fixers because these species can potentially benefit from N acquired through N-fixation.

MAOM data

We retrieved data on MAOM and particulate organic matter for the subset of studies employing size or density fractionation of soil organic matter ($n = 19$). Because of methodological differences, particulate organic matter is loosely defined as organic matter recovered in the total coarse (typically >53 µm) or light (typically <1.6 g cm^{-3}) soil fraction. Where MAOM was not reported, it was estimated based on mass balance by subtracting the particulate organic matter fraction from total C.

FACE-MDS

We use data from the FACE MDS Project Phase 2[34,57–61], in which 12 models were applied to six eCO_2 experiments. Each model covered the time periods representative of the FACE experiments, following a standardized protocol including meteorological forcing, CO_2 concentration, site history and vegetation characteristics for each site.

Experiments included in the FACE-MDS Project Phase 2 were Duke FACE[62], Kennedy Space Center[63], Nevada Desert FACE[64], Oak Ridge FACE[38], Prairie PHACE[65,66] and Rhinelander[67]. Models included were CLM4.0[68], CLM4.5, DAYCENT, CABLE, JULES[69], LPJ-GUESS, OCN, TECO, ORCHIDEE[70], GDAY, ISAM, and SDGVM. See ref. [60] for an overview of model structures and processes. As in the observational data, we compared relative changes in aboveground biomass and SOC stocks of each experiment for eCO_2 relative to control treatments.

TRENDY models

We use model outputs from the TRENDY version 7 S1 simulations, where each model is driven by standardized forcings of observed increasing CO_2 for the years 1700–2018, and constant preindustrial climate and land use. We selected six models that provided outputs for aboveground vegetation carbon (taken as the sum of wood and leaf carbon), SOC and net primary productivity (CABLE-POP[71], CLM5.0[72], ISAM[73], LPJ-GUESS[74], ORCHIDEE[70] and ORCHIDEE-CNP[75]). Wood carbon often includes coarse roots in models. Here, we evaluate relative changes and numbers are not sensitive to the exact definition. Description of models can be found in ref. [76]. Briefly, ORCHIDEE-CNP includes an interactive N and phosphorus cycle, whereas ORCHIDEE is a C-only model. The rest have coupled C–N cycles. Relative changes were calculated based on means over ten initial years (i, varying depending on the model) and $j = 2008–2017$ as $(C_j - C_i)/C_i$. To reduce effects of discrepant response timescales of soil C and biomass, we estimated the steady-state soil C storage (C*) as:

$$C^* = \frac{C_j}{1 - \frac{\Delta C_j}{NPP_j}},$$

where ΔC_j is the change in soil C over the years 2008–2017. The relative change in soil C is then taken as $(C^* - C_i)/C_i$. Data shown in Fig. 4 is based on pooled data from all six models. We randomly sampled outputs from n gridcells for each model in order not to bias the visualization towards models with a large number of gridcells (that is, higher resolution). Here n is chosen as the number of gridcells in the model with the coarsest resolution.

Expected β_{soil} from CMIP5 models

We used projected SOC (C_{soil}) and biomass pool (C_{veg}) responses to rising CO_2 as simulated by CMIP5 models as a comparison for the scaled-up values we derive from experiments. Specifically, we used data from the experiment 'esmFixClim1', in which CO_2 is increased by 1% per year from 285 ppm. In the esmFixClim1 experiment, the increase in $[CO_2]$ affects only vegetation and not the radiation code of the models, enabling a quantification of the effect of eCO_2 in isolation (for example, excluding warming), and thus a close comparison with eCO_2 experiments. At a $[CO_2]$ increasing rate of +1% yr^{-1}, $[CO_2]$ reaches 372 ppm (average concentration in ambient CO_2 plots in the dataset) in the 28th year and 616 ppm (average concentration in elevated CO_2 plots in the dataset) in the 78th year. ΔC_{veg} and ΔC_{soil} were calculated as the difference between the respective carbon stocks in the 28th and the 78th year.

Although plants in both experiments and our CMIP5 dataset see a similar increase in $[CO_2]$, experiments simulate a step increase in CO_2 over half a decade, whereas the increase in CO_2 in CMIP5 models is much slower and occurs over the course of 50 years (Extended Data Table 2). As soil organic matter turns over slowly, the resulting β_{soil} from experiments is lower than ΔC_{soil} from models, and the comparison is not meaningful. We thus focus on the specific relationship β_{plant}:β_{soil} in experiments versus models. Here, we calculated the spatially explicit ratio of $\Delta C_{veg(CMIP)}$ to $\Delta C_{soil(CMIP)}$. This was done for five Earth system models in the CMIP5 ensemble with esmFixClim1 simulations (CanESM2; GFDL-ESM2M; HadGEM2-ES; IPSL-CM5A-LR; and MPI-ESM-LR). Then, we calculate the 'expected' β_{soil} (in units of megagrams of C per hectare) from CMIP5, applying the same β_{plant} used for experiments with the model-average $\Delta C_{veg(CMIP)}$ to $\Delta C_{soil(CMIP)}$ ratio, as follows: $\beta_{plant} \times \Delta C_{soil(CMIP)}/\Delta C_{veg(CMIP)}$, where β_{plant} represents the effect of elevated CO_2 on plant biomass derived from eCO_2 experiments. We then computed the difference between the expected (modelled) and observed (scaled up) effects of elevated CO_2 on β_{soil}. As both expected and scaled-up β_{soil} use the same β_{plant}, this transformation allows us to tackle the consequences of the different $\beta_{soil}/\beta_{plant}$ ratios between experiments and

models directly. We acknowledge, however, that the ratio is likely to change over time, so the comparison needs to be interpreted with caution. We found, however, that first-order models also simulate a positive relationship between β_{soil} and β_{plant} when forced to simulate over the same duration as experiments (Fig. 4a), suggesting that the sign of the β_{soil}:β_{plant} relationship in CMIP5 models would probably not reverse if CMIP5 models were forced to simulate a step increase in CO_2 over 5 yr, as in experiments.

Data availability

All the empirical data that support the main findings of this study have been deposited in Figshare (https://figshare.com/projects/Effects_of_elevated_CO_2_on_soil_and_ecosystem_carbon_storage/74721) and GitHub (https://github.com/cesarterrer/SoilC_CO_2). FACE-MDS data can be accessed at https://www.osti.gov/dataexplorer/biblio/dataset/1480327. CMIP5 data can be accessed at https://esgf-index1.ceda.ac.uk/search/cmip5-ceda/. TRENDY data can be requested at http://dgvm.ceh.ac.uk/index.html.

Code availability

The R code used in the analysis presented in this paper is available in GitHub and can be accessed at https://github.com/cesarterrer/SoilC_CO_2.

41. Terrer, C. *Report of Mutualistic Associations, Nutrients, and Carbon Under eCO_2 (ROMANCE) v1.0 Dataset*. https://doi.org/10.6084/m9.figshare.11704491.v7 (2020).
42. Dieleman, W. I. J. et al. Simple additive effects are rare: a quantitative review of plant biomass and soil process responses to combined manipulations of CO_2 and temperature. *Glob. Change Biol.* **18**, 2681–2693 (2012).
43. Borenstein, M., Hedges, L. V., Higgins, J. P. T. & Rothstein, H. R. in *Introduction to Meta-Analysis* 225–238 (John Wiley & Sons, 2009).
44. Del Re, A. C. & Hoyt, W. T. MAd: meta-analysis with mean differences. *R Package Version 08-2* https://cran.r-project.org/package=MAd (2014).
45. Song, J. & Wan, S. *A Global Database Of Plant Production And Carbon Exchange From Global Change Manipulative Experiments* https://doi.org/10.6084/m9.figshare.7442915.v9 (2020).
46. Viechtbauer, W. Conducting meta-analyses in R with the metafor Package. *J. Stat. Softw.* **36**, https://doi.org/10.18637/jss.v036.i03 (2010).
47. Osenberg, C. W., Sarnelle, O., Cooper, S. D. & Holt, R. D. Resolving ecological questions through meta-analysis: goals, metrics, and models. *Ecology* **80**, 1105–1117 (1999).
48. Rubin, D. B. & Schenker, N. Multiple imputation in health-are databases: an overview and some applications. *Stat. Med.* **10**, 585–598 (1991).
49. Lajeunesse, M. J. Facilitating systematic reviews, data extraction and meta-analysis with the METAGEAR package for R. *Methods Ecol. Evol.* **7**, 323–330 (2016).
50. Van Lissa, C. J. MetaForest: exploring heterogeneity in meta-analysis using random forests. Preprint at https://psyarxiv.com/myg6s/ (2017).
51. Kuhn, M. Building predictive models in R using the caret package. *J. Stat. Softw.* **28**, https://doi.org/10.18637/jss.v028.i05 (2008).
52. Calcagno, V. & de Mazancourt, C. glmulti: an R package for easy automated model selection with (generalized) linear models. *J. Stat. Softw.* **34**, https://doi.org/10.18637/jss.v034.i12 (2010).
53. van Groenigen, K. J. et al. Element interactions limit soil carbon storage. *Proc. Natl Acad. Sci. USA* **103**, 6571–6574 (2006).
54. Wang, B. & Qiu, Y. L. Phylogenetic distribution and evolution of mycorrhizas in land plants. *Mycorrhiza* **16**, 299–363 (2006).
55. Maherali, H., Oberle, B., Stevens, P. F., Cornwell, W. K. & McGlinn, D. J. Mutualism persistence and abandonment during the evolution of the mycorrhizal symbiosis. *Am. Nat.* **188**, E113–E125 (2016).
56. Terrer, C., Vicca, S., Hungate, B. A., Phillips, R. P. & Prentice, I. C. Mycorrhizal association as a primary control of the CO_2 fertilization effect. *Science* **353**, 72–74 (2016).
57. Medlyn, B. E. et al. Using ecosystem experiments to improve vegetation models. *Nat. Clim. Chang.* **5**, 528–534 (2015).
58. Zaehle, S. et al. Evaluation of 11 terrestrial carbon–nitrogen cycle models against observations from two temperate Free-Air CO_2 Enrichment studies. *New Phytol.* **202**, 803–822 (2014).
59. De Kauwe, M. G. et al. Where does the carbon go? A model-data intercomparison of vegetation carbon allocation and turnover processes at two temperate forest free-air CO_2 enrichment sites. *New Phytol.* **203**, 883–899 (2014).
60. Walker, A. P. et al. Comprehensive ecosystem model-data synthesis using multiple data sets at two temperate forest free-air CO_2 enrichment experiments: model performance at ambient CO_2 concentration. *J. Geophys. Res. Biogeosci.* **119**, 937–964 (2014).
61. Walker, A. P. et al. Decadal biomass increment in early secondary succession woody ecosystems is increased by CO_2 enrichment. *Nat. Commun.* **10**, 454 (2019).
62. Schlesinger, W. et al. in *Managed Ecosystems and CO_2* 197–212 (2006).
63. Hungate, B. A. et al. Cumulative response of ecosystem carbon and nitrogen stocks to chronic CO_2 exposure in a subtropical oak woodland. *New Phytol.* **200**, 753–766 (2013).
64. Jordan, D. N. et al. Biotic, abiotic and performance aspects of the Nevada Desert Free-Air CO_2 Enrichment (FACE) Facility. *Glob. Change Biol.* **5**, 659–668 (1999).
65. Carrillo, Y., Dijkstra, F., LeCain, D., Blumenthal, D. & Pendall, E. Elevated CO_2 and warming cause interactive effects on soil carbon and shifts in carbon use by bacteria. *Ecol. Lett.* **21**, 1639–1648 (2018).
66. Mueller, K. E. et al. Impacts of warming and elevated CO_2 on a semi-arid grassland are non-additive, shift with precipitation, and reverse over time. *Ecol. Lett.* **19**, 956–966 (2016).
67. Zak, D. R., Pregitzer, K. S., Kubiske, M. E. & Burton, A. J. Forest productivity under elevated CO_2 and O_3: positive feedbacks to soil N cycling sustain decade-long net primary productivity enhancement by CO_2. *Ecol. Lett.* **14**, 1220–1226 (2011).
68. Oleson, K. et al. *Technical Description of Version 4.5 of the Community Land Model (CLM)* Report NCAR/TN-503+STR, https://doi.org/10.5065/D6RR1W7M (2013).
69. Clark, D. B. et al. The Joint UK Land Environment Simulator (JULES), model description—Part 2: Carbon fluxes and vegetation dynamics. *Geosci. Model Dev.* **4**, 701–722 (2011).
70. Krinner, G. et al. A dynamic global vegetation model for studies of the coupled atmosphere-biosphere system. *Glob. Biogeochem. Cycles* **19**, https://doi.org/10.1029/2003GB002199 (2005).
71. Haverd, V. et al. A new version of the CABLE land surface model (subversion revision r4601) incorporating land use and land cover change, woody vegetation demography, and a novel optimisation-based approach to plant coordination of photosynthesis. *Geosci. Model Dev.* **11**, 2995–3026 (2018).
72. Lawrence, D. M. et al. The Community Land Model Version 5: description of new features, benchmarking, and impact of forcing uncertainty. *J. Adv. Model. Earth Syst.* **11**, 4245–4287 (2019).
73. Meiyappan, P., Jain, A. K. & House, J. I. Increased influence of nitrogen limitation on CO_2 emissions from future land use and land use change. *Glob. Biogeochem. Cycles* **29**, 1524–1548 (2015).
74. Smith, B. et al. Implications of incorporating N cycling and N limitations on primary production in an individual-based dynamic vegetation model. *Biogeosciences* **11**, 2027–2054 (2014).
75. Goll, D. S. et al. A representation of the phosphorus cycle for ORCHIDEE (revision 4520). *Geosci. Model Dev.* **10**, 3745–3770 (2017).
76. Friedlingstein, P. et al. Global carbon budget 2019. *Earth Syst. Sci. Data* **11**, 1783–1838 (2019).
77. Harris, I., Jones, P. D., Osborn, T. J. & Lister, D. H. Updated high-resolution grids of monthly climatic observations—the CRU TS3.10 dataset. *Int. J. Climatol.* **34**, 623–642 (2014).
78. Soudzilovskaia, N. A. et al. Global mycorrhizal plant distribution linked to terrestrial carbon stocks. *Nat. Commun.* **10**, 5077 (2019).
79. Hengl, T. et al. SoilGrids250m: global gridded soil information based on machine learning. *PLoS One* **12**, e0169748 (2017).
80. Batjes, N. H. Harmonized soil property values for broad-scale modelling (WISE30sec) with estimates of global soil carbon stocks. *Geoderma* **269**, 61–68 (2016).
81. Shangguan, W., Dai, Y., Duan, Q., Liu, B. & Yuan, H. A global soil data set for earth system modeling. *J. Adv. Model. Earth Syst.* **6**, 249–263 (2014).

Acknowledgements We thank C. Körner, R. Norby, M. Schneider, K. Treseder, M. Hoosbeek and others for sharing data and advice. We thank the TRENDY, CMIP5 and FACE-MDS teams for the provision of the model simulations. C.T. was supported by a Lawrence Fellow award through Lawrence Livermore National Laboratory (LLNL). This work was performed under the auspices of the US Department of Energy by LLNL under contract DE-AC52-07NA27344 and was supported by the LLNL-Laboratory Directed Research and Development (LDRD) programme under project number 20-ERD-055. J.B.F. contributed to this research from the Jet Propulsion Laboratory, California Institute of Technology, under a contract with the National Aeronautics and Space Administration. Government sponsorship acknowledged. Funding provided in part by the NASA Interdisciplinary Science (IDS) programme, and by the US Department of Energy, Office of Science, Office of Biological and Environmental Research, Terrestrial Ecosystem Science Program under Award Numbers DE-SC0008317, DE-SC0016188 and the LLNL Soil Science Focus Area (SFA) SCW1632. B.A.H. and K.J.v.G. were supported by the US Department of Energy through the Terrestrial Ecosystem Science Program DE-SC0010632. The FACE Model-Data Synthesis was supported by the US Department of Energy, Office of Science, Biological and Environmental Research programme. Oak Ridge National Laboratory is operated by UT-Battelle LLC under contract DE-AC05-00OR22725 with the US Department of Energy. The BioCON experiment was funded by the Long-Term Ecological Research (LTER) grants DEB-0620652, DEB-1234162 and DEB-1831944, Long-Term Research in Environmental Biology (LTREB) grants DEB-1242531 and DEB-1753859, Biological Integration Institutes grant NSF-DBI-2021898, Ecosystem Sciences grant DEB-1120064, and Biocomplexity grant DEB-0322057, and by the US Department of Energy Programs for Ecosystem Research grant DE-FG02-96ER62291.

Author contributions C.T. and R.P.P. conceived the original idea. C.T. designed the paper, with R.B.J., B.A.H. and K.J.v.G. contributing to the development of the conceptual framework. J.R. and C.T. collected the biomass and SOC data for the experiments. M.C. collected MAOM data. K.V.S. and S.V. collected litter data. C.T. ran the statistical analyses and scaling up. B.D.S. ran the analysis with TRENDY models. B.N.S., C.T. and B.A.H. ran the comparison with the FACE-MDS data. T.F.K., H.Z. and C.T. analysed CMIP5 data. P.B.R., B.A.H., E.P., Y.C., R.D.E, R.B.J. and many others ran the experiments. C.T. and B.A.H. wrote the first draft, with input from all authors.

Competing interests The authors declare no competing interests.

Additional information

Supplementary information The online version contains supplementary material available at https://doi.org/10.1038/s41586-021-03306-8.

Correspondence and requests for materials should be addressed to C.T.

Peer review information *Nature* thanks Jonathan Sanderman and the other, anonymous, reviewer(s) for their contribution to the peer review of this work. Peer reviewer reports are available.

Reprints and permissions information is available at http://www.nature.com/reprints.

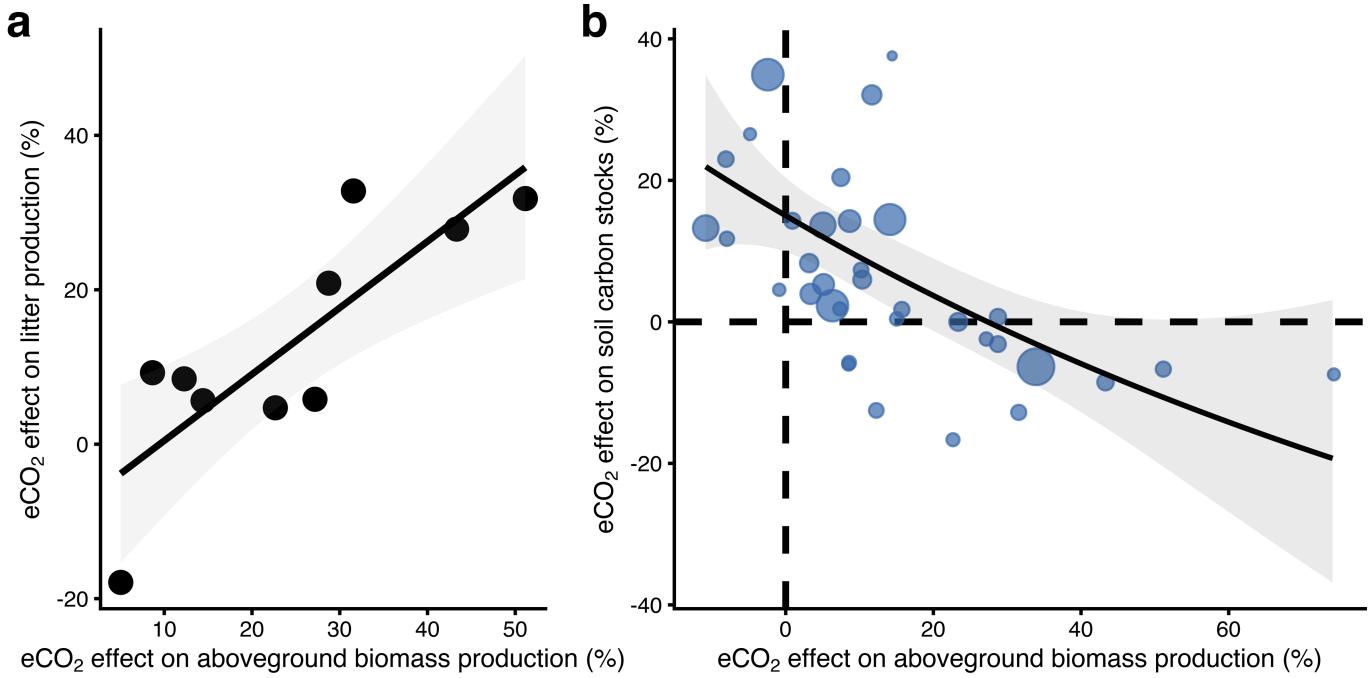

Extended Data Fig. 1 | Effects of eCO_2 on aboveground biomass production versus effects of eCO_2 on litter production and SOC storage. a, Effect of eCO_2 on litter production as the effect of eCO_2 on aboveground biomass production increases. **b**, Effect of CO_2 on SOC storage as the effect of CO_2 on aboveground biomass production increases. Results for non-fertilized field eCO_2 experiments ($n = 10$, and $n = 35$, respectively). Grey shading around regression lines represents the 95% confidence intervals. Dots represent individual experiments, with dot size in **b** proportional to the weights in the meta-regression.

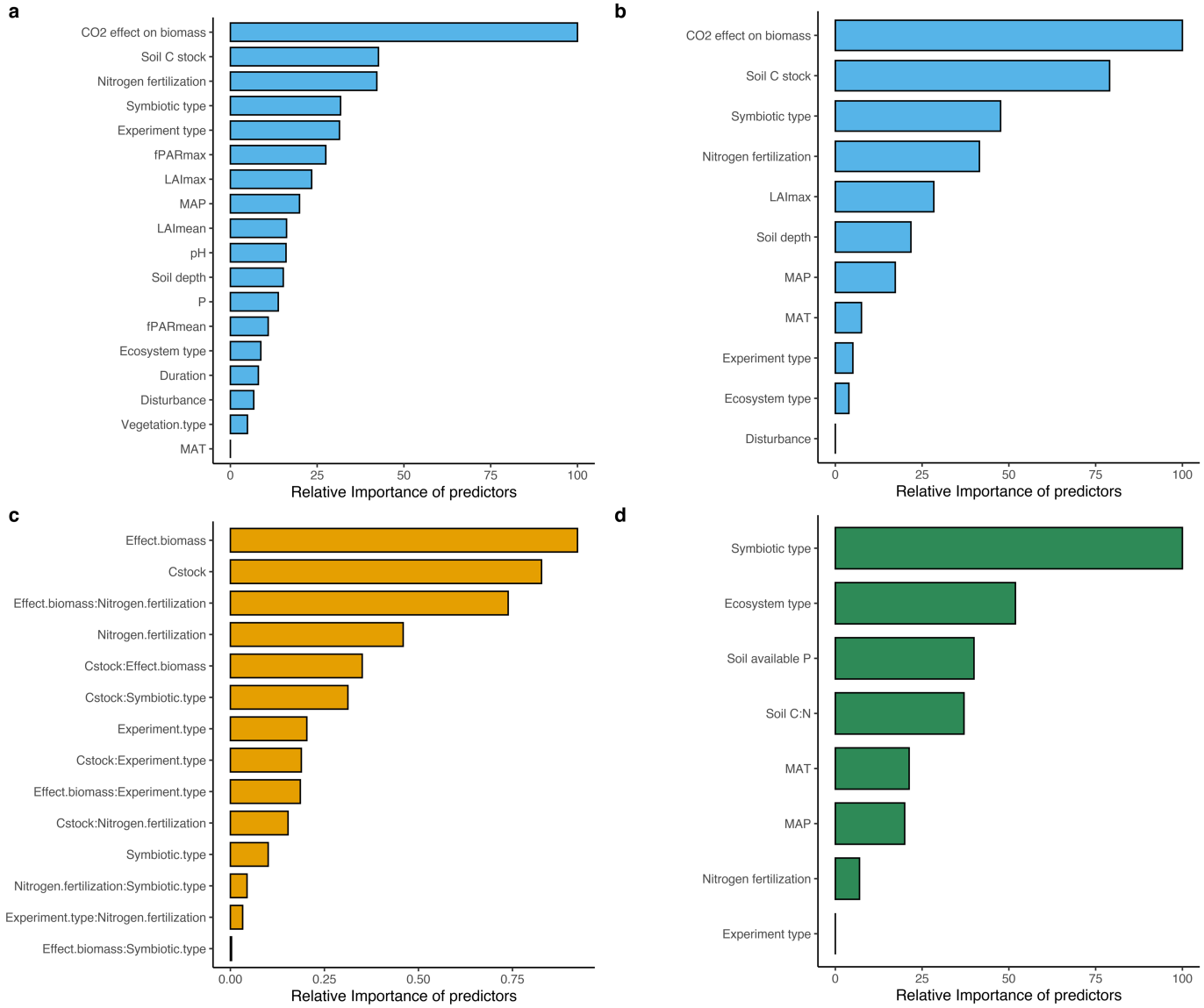

Extended Data Fig. 2 | Variable importance of 19 predictors of the effects of CO_2 on SOC and biomass stocks. a, **b**, Varying importance of the effect of CO_2 on SOC stocks in relative (**a**) and absolute terms (**b**) across the full dataset ($n = 108$). **c**, Varying importance of the effect of CO_2 on SOC stocks (%) across the subset of eCO_2 experiments in 'intact' soils ($n = 73$). **d**, Varying importance of the effect of CO_2 on plant aboveground biomass ($n = 138$). The varying importance in **a**, **b** and **d** is quantified based on a meta-forest model. The varying importance in **c** is quantified based on the sum of AICc weights, which allows for the quantification of the importance of interactions between predictors. As an initial step, moderators that consistently displayed negative variable importance (that is, that showed a reduction in predictive performance) were automatically dropped. LAImax, LAImean, MAP and MAT are defined in Extended Data Table 1.

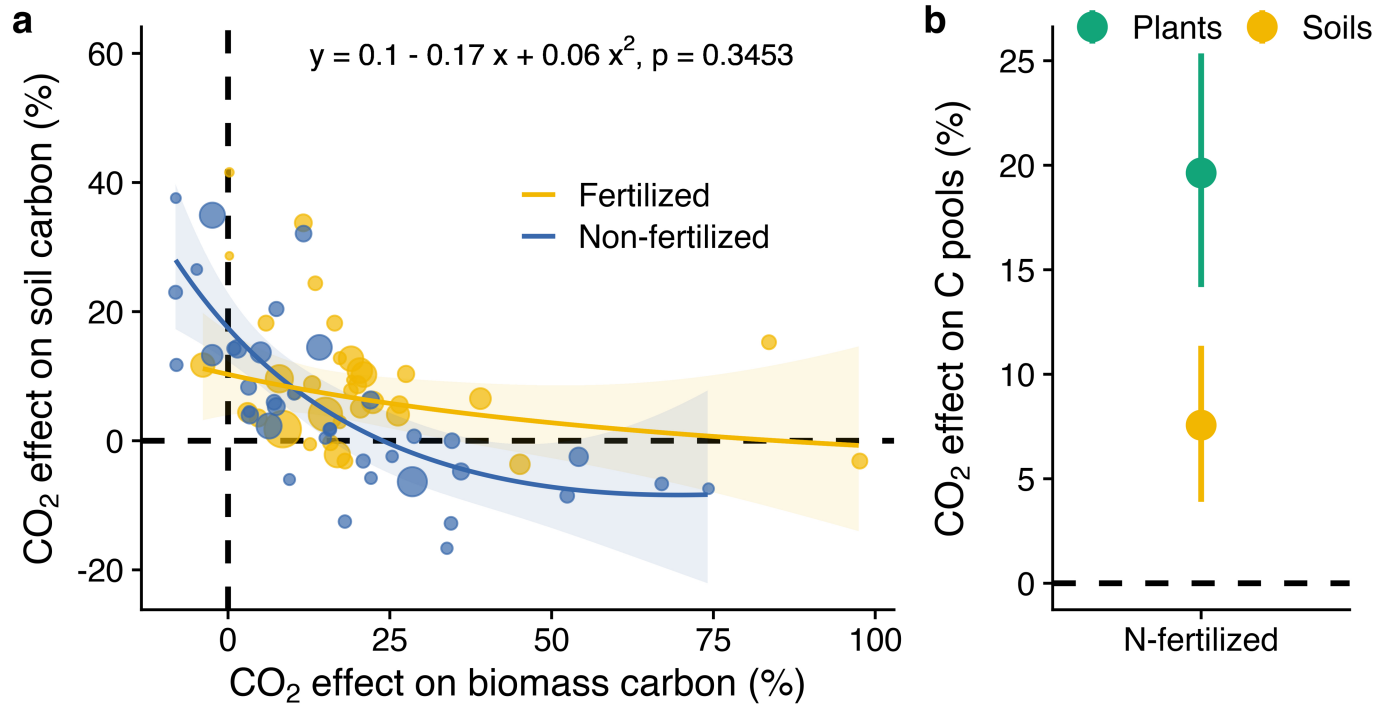

Extended Data Fig. 3 | Effects of eCO_2 on SOC stocks and plant biomass in nitrogen-fertilized eCO_2 studies. $n = 35$. **a**, **b**, Effects are expressed as a regression (**a**) and overall effects in meta-analysis (**b**). Dot sizes in **a** represent the individual studies and are drawn proportional to the weights in the model. The regression with the subset of non-fertilized studies is also shown in **a** for comparison. Dots in **b** represent the effect sizes and 95% confidence intervals from the meta-analysis.

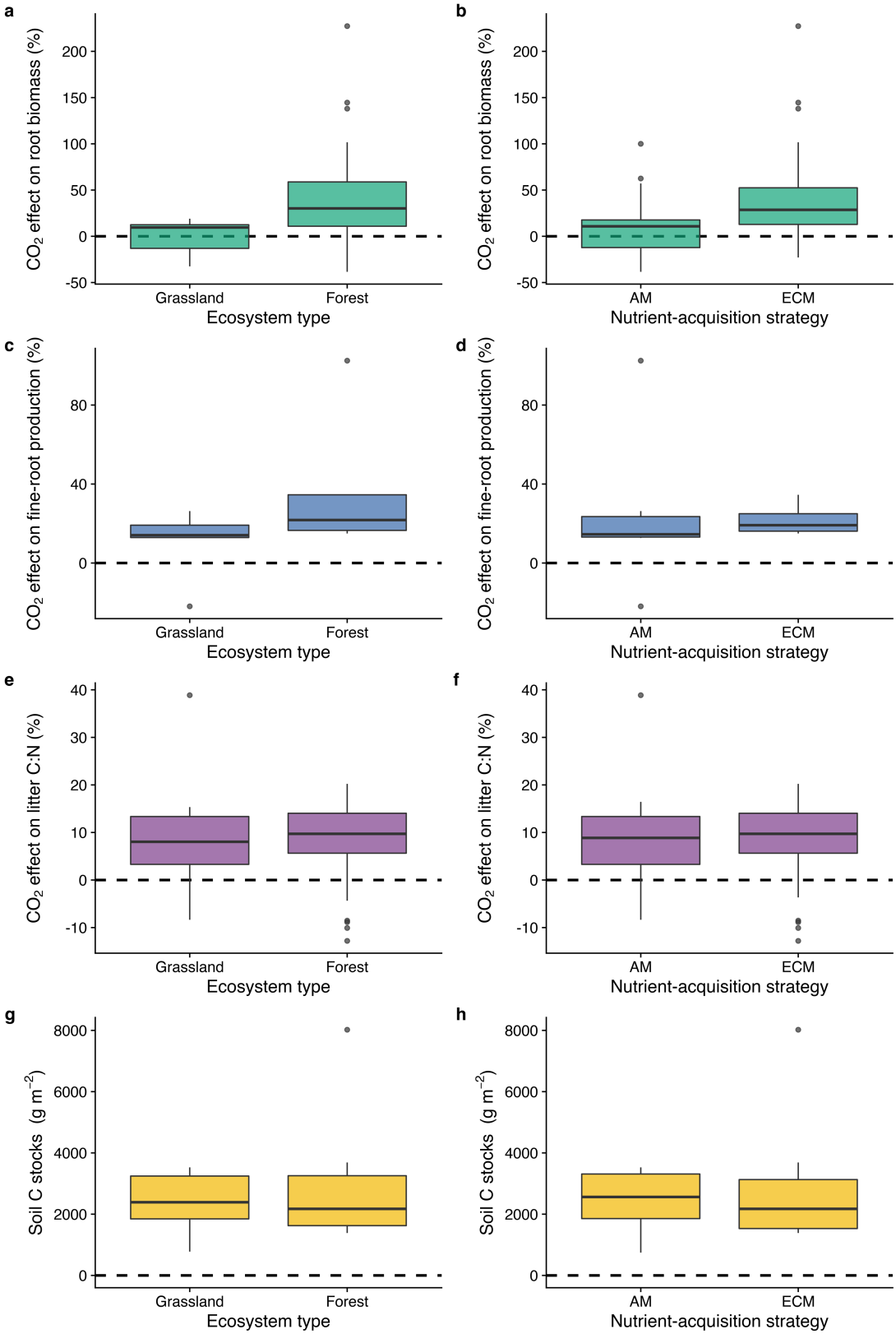

Extended Data Fig. 4 | Analysis of variables potentially explaining the observed effects of eCO_2 on SOC. Effects of eCO_2 on root biomass ($n = 45$), fine-root production ($n = 11$), litter C:N ($n = 16$) and background SOC stocks ($n = 38$), between ecosystem types (grassland versus forest) and nutrient-acquisition strategies (AM versus ECM). Boxplots show the median, the first to third quartile, the 1.5× interquartile ranges, and outliers.

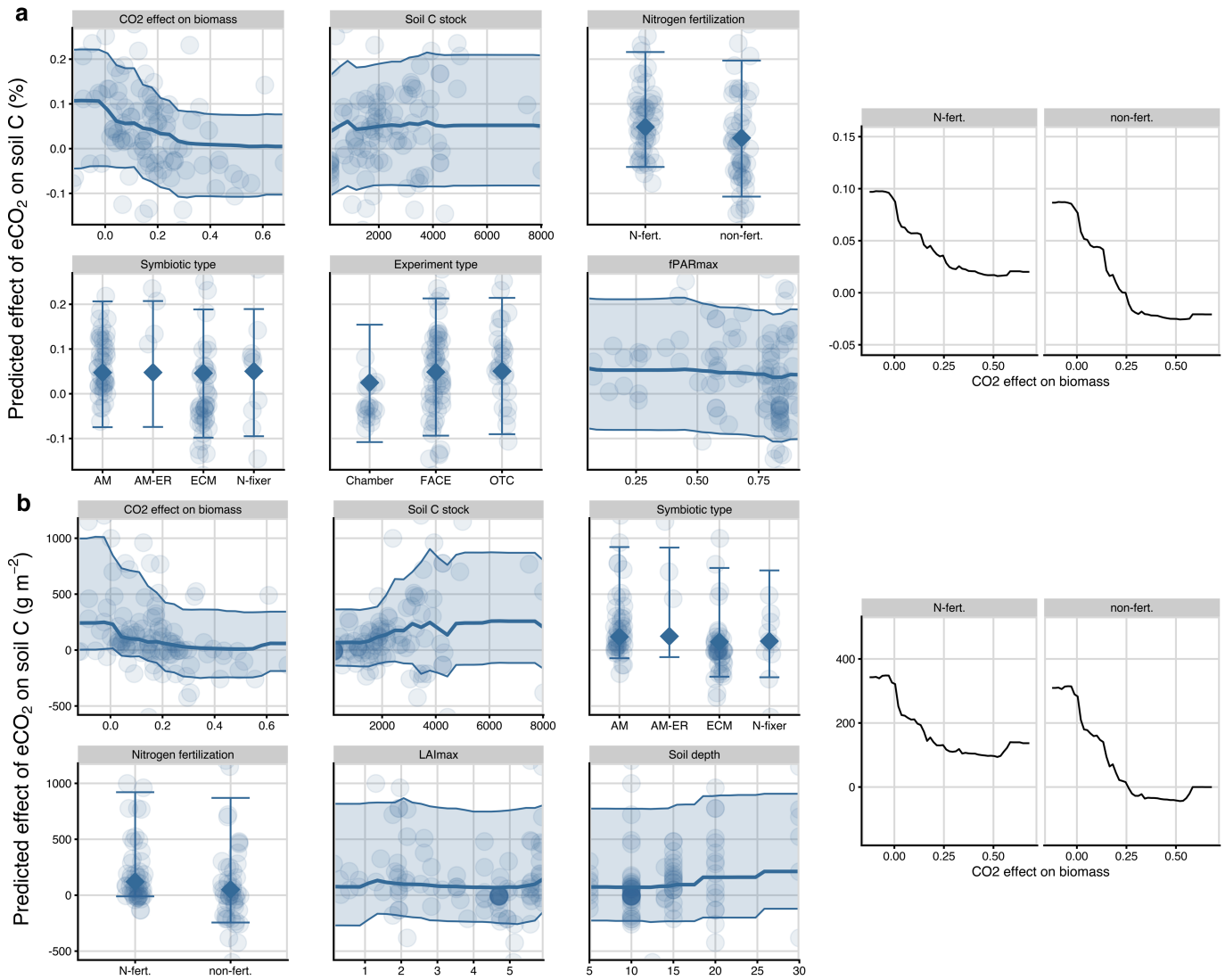

Extended Data Fig. 5 | Partial dependence plots of the six most important predictors of the effect of eCO_2 on SOC stocks across 108 experiments. The figure shows the predicted CO_2 effect in relative (**a**) and absolute terms (**b**) across each predictor and the most important interaction between predictors (right panels) in a random-forest meta-analysis. Error bands represent 95% confidence intervals. Partial regression plots give a graphical depiction of the marginal effect of a variable on the response and the shape and direction of the relationship. Little variation in the predicted effect of eCO_2 across the values of a predictor generally reflects the low predictive power of the predictor. However, important predictors may show little variation in the predicted effect of eCO_2 when involved in interactions, so the right panels show the most important interaction in the model. More details about the different predictors may be found in Extended Data Table 1. From a total of 19 predictors, only the six most important predictors and the most important interaction are shown here.

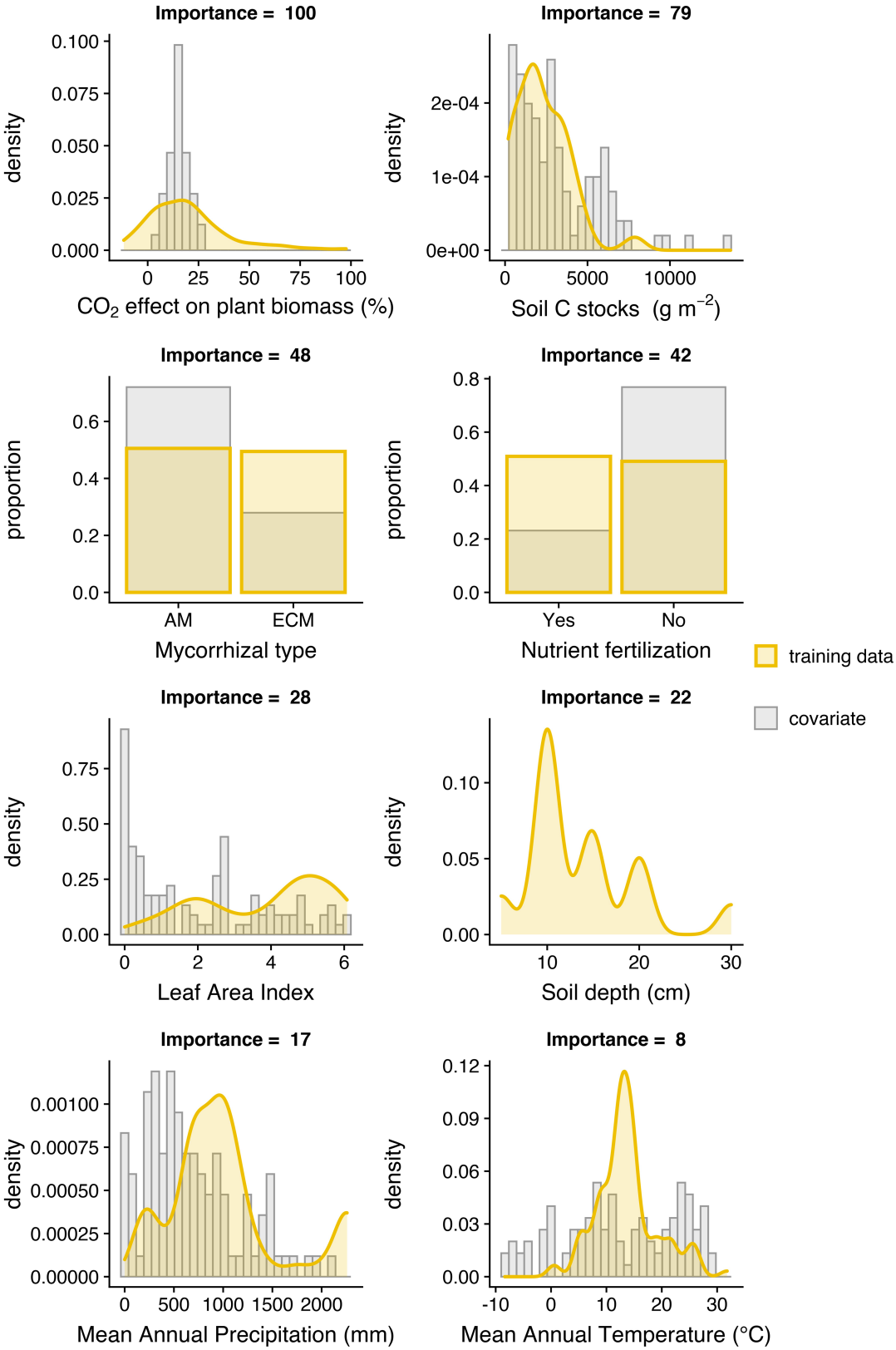

Extended Data Fig. 6 | Representativeness of the scaling-up predictors of the effect of eCO_2 on SOC stocks. Histograms showing the distribution of both the predictors in the training dataset of CO_2 experiments and the data used to scale up the global distribution of the effect. Predictions exclude regions between −15 to 15 and from 60° to 90° latitude owing to the lack of experiments.

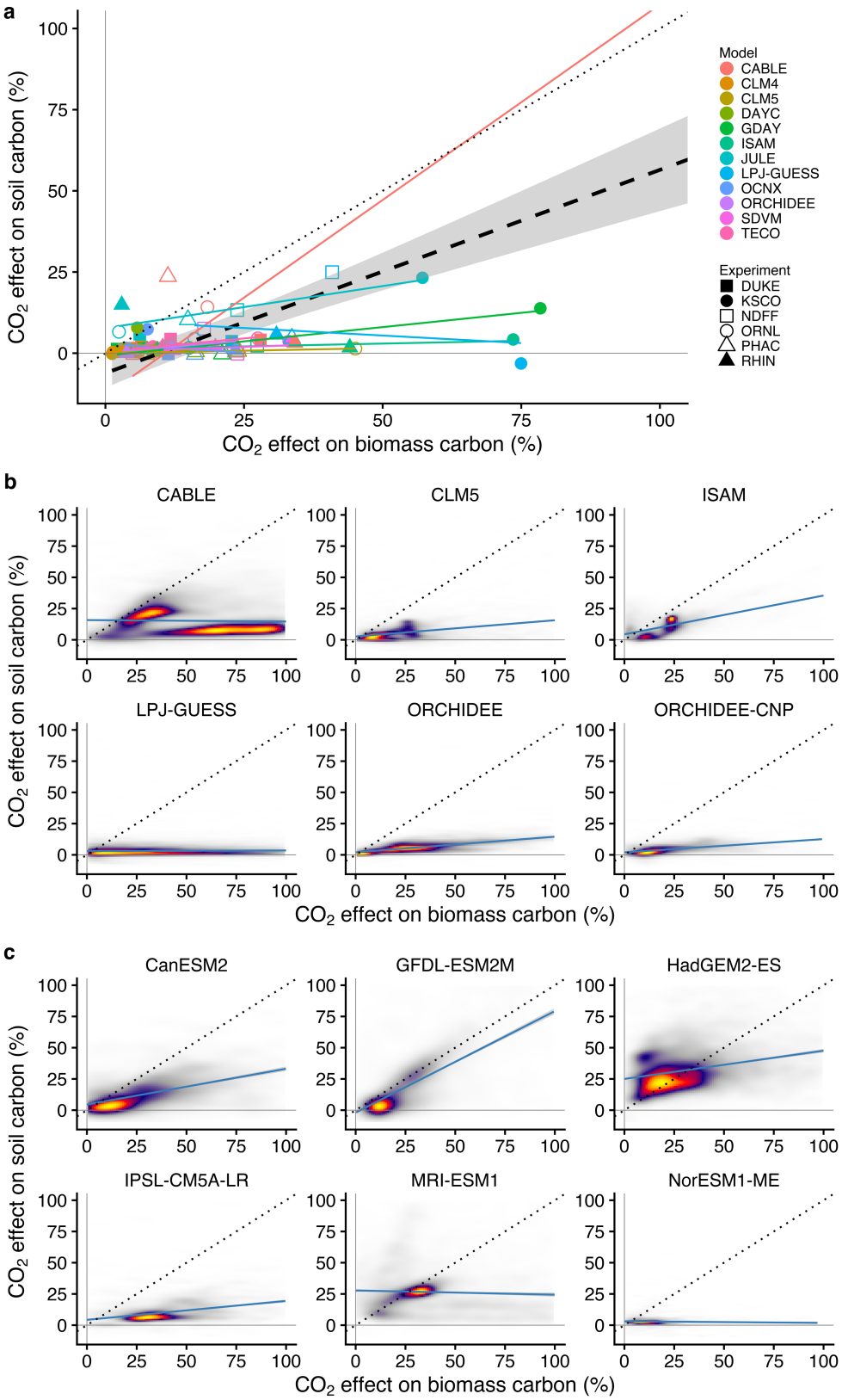

Extended Data Fig. 7 | Relationship between the effects of CO_2 on aboveground biomass and SOC across individual models from three model ensembles. a, FACE Model Data Synthesis Phase 2. Individual model results are represented by coloured symbols and lines. Each symbol represents one site; lines represent model-specific linear regressions. To ease interpretation of the results and the comparison with Fig. 4, axis limits are set. Dashed lines and error bands (grey shading) represent the linear regression line and standard error across all experiment-by-model results. **b**, TRENDY v7 models. **c**, CMIP5 models.

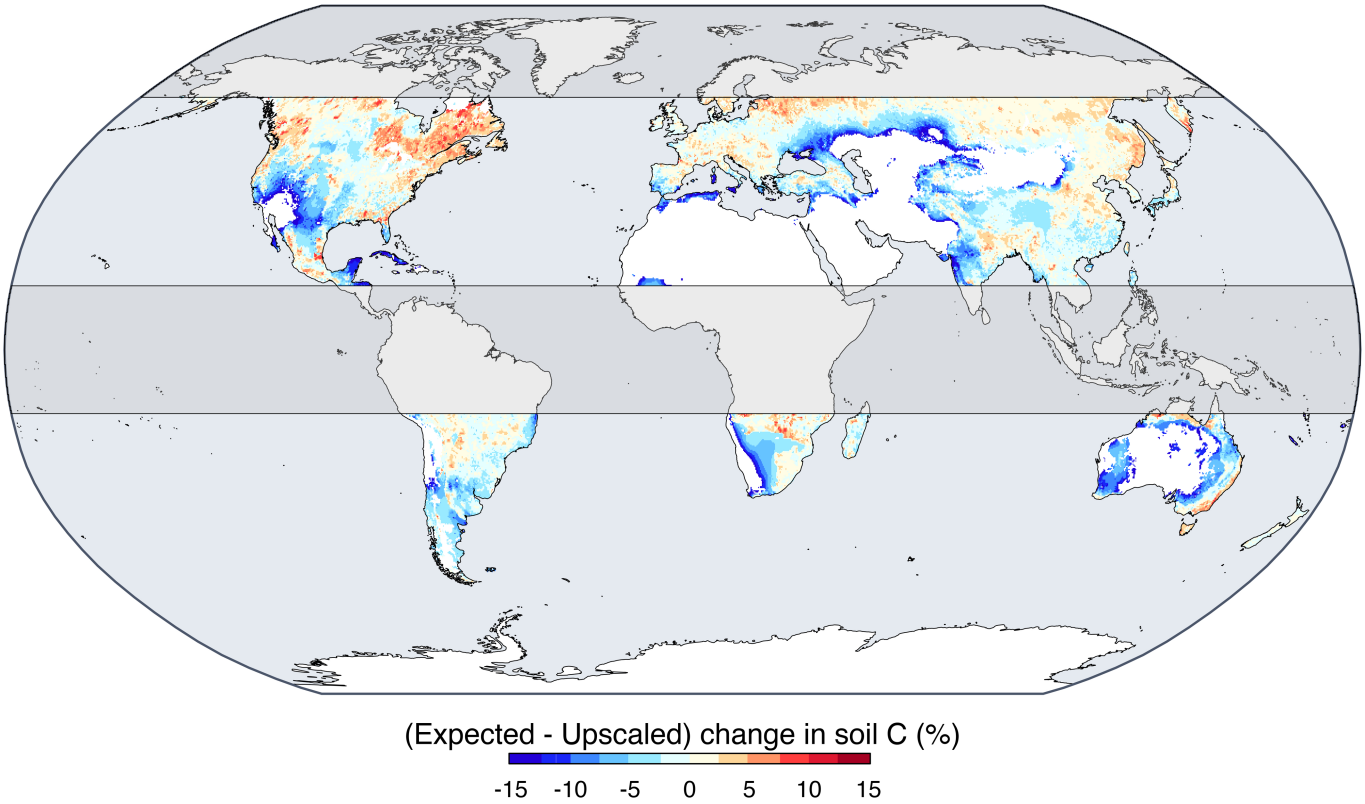

Extended Data Fig. 8 | Difference between expected CO_2 effects on SOC stocks based on TRENDY models and scaled up on the basis of experiments. Expected values result from the relationship between β_{soil} and β_{plant} coded in models. Positive values (red colour) indicate an overestimation by models; negative values (blue colour) indicate an underestimation by models.

Extended Data Table 1 | List of predictors used to examine and to scale up the effects of eCO_2 on SOC

Predictor	Source	Upscaling
Mean annual temperature (MAT)	reported in papers	scaled from CRU[77]
Mean annual precipitation (MAP)	reported in papers	scaled from CRU[77]
Duration of the experiment	reported in papers	non-important
Experiment type	reported in papers	scaled for FACE only
Ecosystem type	reported in papers	scaled from ESA land cover: http://maps.elie.ucl.ac.be/CCI/viewer/download.php
Vegetation type	reported in papers	non-important
Symbiotic type	reported in papers	scaled from ref[78]
Effect of elevated CO_2 on plant biomass	reported in papers	scaled from ref[12]
Disturbance	reported in papers	scaled from ESA land cover: http://maps.elie.ucl.ac.be/CCI/viewer/download.php
Nitrogen fertilization	reported in papers	scaled from ESA land cover: http://maps.elie.ucl.ac.be/CCI/viewer/download.php
Soil carbon stock in control plot	reported in papers	scaled from ref[79]
Soil depth of carbon measurements	reported in papers	scaled for 0-30 cm depth
Soil C:N ratio	[80]	[80]
Soil pH	[79]	Non-important
Soil available P	[81]	[81]
Maximum Leaf Area Index (LAImax)	1 km year 2012 v2 land.copernicus.eu/global/products/lai	land.copernicus.eu/global/products/lai
Mean Leaf Area Index (LAImean)	1 km year 2012 v2	non-important
Maximum fraction of absorbed photosynthetically active radiation (fPARmax)	1 km year 2012 v2 land.copernicus.eu/global/products/fapar	land.copernicus.eu/global/products/fapar
Mean fraction of absorbed photosynthetically active radiation (fPARmean)	1 km year 2012 v2	non-important

Data for each experiment ('reported in papers') was extracted from the references in Supplementary Table 1. Data are from refs. [12,77–81].

Extended Data Table 2 | Synthetic description of the basic characteristics of three model ensembles in terms of their treatment of CO_2 effects

Model ensemble	Spatial extent	CO_2 concentration	Time CO_2 exposure	CO_2 increase
FACE-MDS 2	Site-level (6 sites)	From current levels to elevated CO_2 ("future")	~ 10 years	Step increase
TRENDY v7 S1	Global	From preindustrial levels to current CO_2 ("historical")	1700-2018	Gradual
CMIP5 esmFixClim1	Global	From current levels to elevated CO_2 ("future")	50 years	Gradual
Experiments	**Site-level**	**From current levels to elevated CO_2 ("future")**	**~ 1-10 years**	**Step increase**